

Lawrence Berkeley National Laboratory

LBL Publications

Title

Method—Using Microelectrodes to Explore Solid Polymer Electrolytes

Permalink

<https://escholarship.org/uc/item/9bf1g2sf>

Journal

Journal of The Electrochemical Society, 168(5)

ISSN

0013-4651

Authors

Petrovick, John G
Anderson, Grace C
Kushner, Douglas I
[et al.](#)

Publication Date

2021-05-01

DOI

10.1149/1945-7111/abee5f

Peer reviewed

OPEN ACCESS

Method—Using Microelectrodes to Explore Solid Polymer Electrolytes

To cite this article: John G. Petrovick *et al* 2021 *J. Electrochem. Soc.* **168** 056517

View the [article online](#) for updates and enhancements.



240th ECS Meeting

Oct 10-14, 2021, Orlando, Florida

**Register early and save
up to 20% on registration costs**

Early registration deadline Sep 13

REGISTER NOW





Method—Using Microelectrodes to Explore Solid Polymer Electrolytes

John G. Petrovick,^{1,2,*} Grace C. Anderson,^{1,2,*} Douglas I. Kushner,^{2,**} Nemanja Danilovic,^{2,**} and Adam Z. Weber^{2,***,z}

¹Department of Chemical and Biomolecular Engineering, University of California, Berkeley, California 94720, United States of America

²Energy Technologies Area, Lawrence Berkeley National Laboratory, Berkeley, California 94720, United States of America

Solid polymer electrolytes are an emerging technology in electrochemistry driven by their use in energy applications such as fuel cells, electrolyzers, and solid-state batteries. Compared to traditional liquid electrolytes, solid polymer electrolytes provide safer, cheaper, and potentially improved device performance. However, there is a lack of standard experimental methods for studying solid electrolytes. Microelectrodes have inherent benefits capable of filling this experimental gap due primarily to their integration into model electrochemical cells with solid electrolytes that represent complex interfaces, enabling additional insight into reaction processes. In this tutorial review, we explore the use of microelectrodes to study solid polymer electrolytes, beginning with a brief history of the field including common experimental cell designs and their benefits and drawbacks. Methods of evaluating essential kinetic and mass-transport parameters are then examined. In addition, the key studies of the past 30 years utilizing microelectrode cells and solid polymer electrolytes are summarized, with important results highlighted and compared. Finally, future studies of solid polymer electrolytes with microelectrodes and potential new avenues of research are commented on.

© 2021 The Author(s). Published on behalf of The Electrochemical Society by IOP Publishing Limited. This is an open access article distributed under the terms of the Creative Commons Attribution 4.0 License (CC BY, <http://creativecommons.org/licenses/by/4.0/>), which permits unrestricted reuse of the work in any medium, provided the original work is properly cited. [DOI: 10.1149/1945-7111/abee5f]



Manuscript submitted January 4, 2021; revised manuscript received March 8, 2021. Published May 20, 2021.

Electrochemistry is an essential field of chemistry that is coming to prominence as it enables widespread renewable energy and deep decarbonization across numerous industrial sectors through the use of electrical/chemical energy-conversion and -storage devices. In particular, many of these devices now are solid-state systems, wherein traditional electrochemical techniques are not as readily available for exploration of the governing phenomena. In addition, it is now recognized how important the electrochemical interface plays in such technologies. For example, the reaction interface remains uninterrogated in model systems for devices that utilize polymer electrolytes, such as perfluorosulfonic membranes (PFSA, e.g. Nafion[®]) for proton-exchange-membrane fuel cells (PEMFCs) and water electrolyzers (PEMWEs), or complex oxide ceramics for all solid-state batteries (lithium polysulfate (LPS), lithium lanthanum zirconate garnet (LLZO)). Emblematic of these issues are the exemplary and ubiquitous oxygen reduction and evolution (ORR and OER) and hydrogen oxidation and evolution (HOR and HER) reactions, shown in Fig. 1 and Table I. A gap exists between what can be fundamentally studied about ORR or HOR between a platinum electrode and oxygen or hydrogen-saturated aqueous acids and the behavior of ORR in a fuel cell (membrane electrode assembly, MEA) where the ORR or HOR occurs with interaction between a Nafion ionomer, platinum electrocatalyst, and humidified reactant gas. There are both kinetic and thermodynamic implications to this gap and it is important to have tools to study them.

The study of reaction kinetics in aqueous solutions is conventionally accomplished using the rotating disk electrode (RDE). The RDE was invented by Ivanov and Levich in 1959, alongside the governing equations of hydrodynamics and the convective-diffusion equations.^{1,2} The RDE consists of a disk electrode, typically 5–6 mm in diameter embedded in inert collets made of PTFE or PEEK. The disk, which represents the working electrode, can be polycrystalline metal or oxide, single crystal (with the use of a hanging meniscus collet), glassy carbon, or other inert substrates onto which nanoparticles are drop cast. The collet is screwed into a shaft that can be rotated at a desired rotation rate. RDE equipment is largely available

commercially, as well as custom-made electrode disks of various materials. The premise of the RDE is that, as it rotates, the bottom of the disk drags the solution radially away from the center, and the fluid is replenished by a normal flow to the surface. Depending on the rotation rate, the diffusion layer thickness is also changed in a prescribed manner thus allowing more reactant to be predictably presented to the working electrode disk, producing a higher limiting current. In other words, the mass-transport limiting current of ORR or HOR can be varied by varying the rotation rate. The RDE is an ideal method for studying ORR and HOR reaction mechanisms, catalyst activities, and stability, with the caveat being that the local environment in RDE is aqueous and thus different than in a PEMFC MEA. This introduces multiple issues, including uncertainty regarding interfacial phenomena, reactant solubility limitations, differences in local and bulk pH, and transport limitations in different media. Solubility is especially prevalent for reactions such as CO₂ or CO reduction.^{3,4}

Performing electrochemistry in solid polymer electrolytes has largely been isolated to MEAs consisting of two heterogeneous porous electrodes that are typically greater than 1 cm² geometric area. The electrodes are deposited on the membrane or on gas-diffusion layers and are placed on either side of the solid electrolyte, effectively sandwiching the electrolyte. Most polymer electrolytes require hydration (typically using water vapor), and a solid reproducible electrical/ionic contact must be maintained between the solid electrolyte and the working and counter electrodes to manage the electrolyte resistance. The resulting environment is much more complex and heterogeneous compared to the RDE environments in aqueous electrolyte cells. However, such a cell allows for interrogation of the solid/solid interface between the electrocatalyst and solid polymer electrolyte, in a manner similar to that in actual devices, where transport to the surface and kinetics couple to limit operation.⁵ An important distinction is that MEAs are two-electrode measurements and with perhaps poorly defined interfaces due to their porous, heterogeneous multicomponent catalyst layers. Also, without a specific reference electrode, although often hydrogen systems will use HOR or HER as a pseudo reference, interpretation of the results is difficult to attribute directly kinetic or transport limitations to either the electrode or membrane. A third electrode can be introduced to better resolve the half-cell reaction parameters in an MEA, but this is not trivial and interpretation is not

*Electrochemical Society Student Member.

**Electrochemical Society Member.

***Electrochemical Society Fellow.

^zE-mail: azweber@lbl.gov

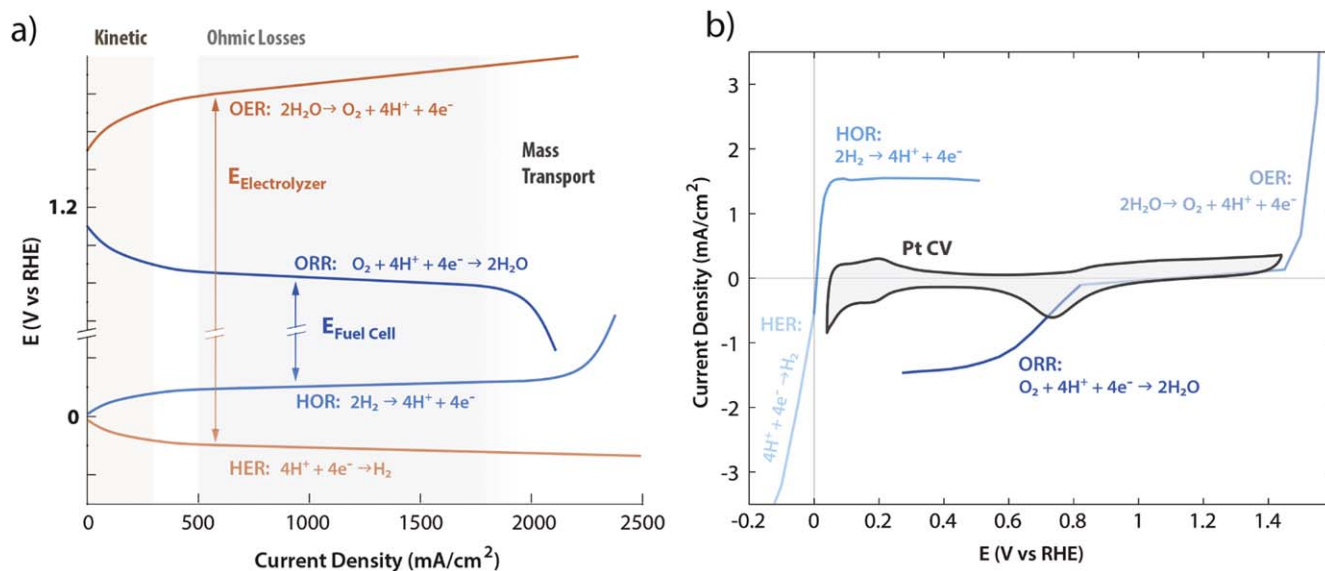


Figure 1. Water based, energy-conversion reactions HOR/HER and OER/ORR viewed as (a) cell level polarization curves schematically and (b) Pt and Ir ME measurements on Nafion solid-polymer electrolyte in humidified room temperature gases.

Table I. Common solid-state electrochemical reactions.

Name	Reaction
Oxygen Reduction	$O_2 + 4H^+ + 4e^- \rightarrow 2H_2O$
Hydrogen Oxidation	$H_2 \rightarrow 2H^+ + 2e^-$
Oxygen Evolution	$2H_2O \rightarrow O_2 + 4H^+ + 4e^-$
Hydrogen Evolution	$2H^+ + 2e^- \rightarrow H_2$

necessarily straightforward due to interactions among the potential fields in the MEA.⁶

Microelectrode (ME) cells are a pathway towards overcoming many limitations associated with MEAs and can represent ideal environments, similar to RDE, that allow for in-depth interrogation of interfacial phenomena.^{7,8} MEs are distinguished as any electrode with a μm scale diameter, while an ultramicroelectrode (UME) is classically defined as any electrode with a geometrically important dimension of $50 \mu\text{m}$ or less.¹ For example, a disk electrode with a diameter less than $50 \mu\text{m}$ would be classified as an UME. The terms will be used interchangeably in the remaining text, as the same general principles apply to both cases. MEs can be formulated in several different geometries, including the aforementioned disk electrode as well as spherical, cylindrical, and band microelectrodes. However, the geometry most used in polymer-electrolyte electrochemistry is the disk electrode due to its ease of manufacture and implementation, and it will be the focus of this paper.⁹ As a result of the field's association with fuel-cell catalysts, platinum (Pt) is by far the most common metal for polymer-electrolyte MEs, but other metals can be used, including gold, iridium, silver, and copper. Iridium would be most appropriate for studying OER, while Pt is more appropriate for HOR, HER, and ORR. For other reactions such as CO₂ reduction or chemical conversions other metals would be more appropriate.⁴

It should be noted that MEs are not limited to solid-state measurements—they can also be used for *in-situ* electrochemical diagnostics. For example, in liquid electrolytes, the small size of MEs results in a very small diffusion layer and low absolute current, reducing the impact of electrolyte resistance, which typically requires compensation in RDE. MEs are also frequently found in the adjacent field of scanning electrochemical microscopy (SECM), which allows for local probing of electrochemical reaction kinetics

at a substrate surface.¹⁰ Many of the experiments detailed later in this work, such as chronoamperometric measurements, are featured heavily in SECM studies, and thus the general principles discussed can be applied in these systems as well.¹¹ MEs have also been used with limited success as sensing electrodes in operating complex devices, where they serve a similar purpose as a given reference electrode. Examples include local chemical sensing in microbial and PEMFCs.^{12,13} However, such applications are nascent and involve more complex phenomena and analysis. Therefore, an in-depth discussion of electrochemical diagnostics is beyond the scope of this work as they are a separate and more specialized use of MEs. Instead, we focus closely on the application of MEs in solid-state setups for kinetic and mass transport analysis.

MEs provide several advantages in solid-state electrochemical applications. For example, they can accommodate stable reference electrodes (dynamic hydrogen electrodes) for treating half-cell electrochemical measurements of kinetics and mass transport similar to RDE half-cells. In addition, the small electrode size lowers the current draw such that ohmic drop is quite small; normally, ohmic drop is a significant concern in more-resistive solid electrolytes (as compared to liquid). However, there are concerns as well; both MEs and RDEs present an ancillary problem in that solution impurities can have a major impact on the result. Additional pros and cons of MEs are presented in Table II, many of which are discussed in more detail later in this work.

The first solid-state ME experiments were accomplished by Appleby and Srinivisan in the 1990s to study ORR using a $100 \mu\text{m}$ Pt ME and a Nafion membrane.^{7,8} The publications cover a multitude of cell design criteria and effects that they found to be important; a handful of other groups have also developed their own unique cells. Interestingly, with only a 20-year gap between RDE and UME development, RDE and MEA testing have become significantly more widespread and common. ME setups for studying this system remain largely difficult for a variety of reasons, including slow equilibration times, overly complex designs, and a reliance on steady-state measurements, as discussed in depth below. In this tutorial, we discuss the appropriate application of MEs including best practices and data analysis as electrochemical diagnostic tools to examine reaction interfaces using as examples the ORR/OER and HOR/HER. First, the cell setup and testing procedures are discussed, followed by general analysis of the experimental data for kinetics and mass transport. Next, applications of MEs are critically reviewed. Finally, summary and future directions are noted.

Table II. Pros and cons of using microelectrodes to study solid-state electrolytes.

Cell Design Features	
Pros	Cons
<ul style="list-style-type: none"> • Effective control of environmental variables, including relative humidity, potential, temperature, and gas flow • Simple, robust design that minimizes layers and interfaces with ideal geometry • Allows for product gas analysis for additional insights into reaction products 	<ul style="list-style-type: none"> • Low currents are significantly affected by room noise, necessitating a Faraday cage • Equilibration times and experiments can be quite lengthy • Avoiding contamination is critical because low currents are easily influenced by even small amounts of contaminant
Experimental Design	
Pros	Cons
<ul style="list-style-type: none"> • A wide range of reactions are available to study, including fuel cell reactions, water splitting, and carbon dioxide reduction • Low ohmic drop ensures accurate current measurements and low overpotentials • Limiting system to one reaction simplifies both kinetics and mass transport phenomena • Allows for accurate transient analysis of current response, something that is difficult with MEA scale devices • Model system that avoids complicated interfaces 	<ul style="list-style-type: none"> • For mass-transport measurements, no analytical solution exists, requiring the use of numerical modeling or analytical approximations • If using thin films, dropcasting the films produces irregular shapes, which can impact measurements and interpretation • At high current density, thin films may peel away from the electrode surface due to repulsive forces and reactant/product consumption/generation

bridge to the reference electrode. This configuration benefits from a polymer layer tightly bound to the ME surface in which external gases are unable to penetrate and react directly at the electrode. An additional benefit to a free-standing configuration is an unimpeded flow of gas to the polymer/air interface, reducing chances of an electrode blocking the pathways of the gases. However, there is difficulty in providing good connectivity between the counter electrode and cast films, as well as the reference electrode bridge acting as a weak point during hydration studies due to detachment. An additional concern involves the slow diffusion of the liquid electrolyte in the reference chamber through the bridge leading to eventual contamination of the film of interest. These two configurations suffer from high sensitivity to environmental condition changes and compromises at the electrode interface: unnecessary surface roughness and chemical contamination.

Precise environmental control plays an important factor when performing measurements, regardless of the configurations used. The most common environments explored in solid-polymer-electrolyte studies involve humidity and gas type/concentration, while some studies have involved temperature and pressure. The simplest condition that can be changed is the gas type to look at the different reactions taking place on the ME as these are typically supplied in a gas cylinder at specific concentrations to the environmental chamber. The next condition involves humidity generated at room temperature by mixing humid air at dew point with a dry air stream at different ratios to target specific relative humidity set points. As more variables are included in the cell design, the complexity of environmental control becomes more difficult. For instance, when temperature is involved, the control of humidity becomes increasingly difficult without proper temperature control and insulation. Humidity is generated by flowing the gas through a water vessel at a set temperature to produce air at dew point. The difference typically seen in practice is that the vapor stream is heated up to the measurement temperature rather than mixed with a dry air stream. If any component drops below the water vessel temperature then condensation forms that will alter the final humidity in the test cell. Lastly, while many studies involve measurements performed under atmospheric pressure, pressure can be increased to allow for studies above 100 °C, but special considerations must be taken into account as performing pressurized experiments can pose a safety hazard.

An additional consideration when working with MEs is the surface roughness of the electrode itself. While the surface of the electrode may be macro- and microscopically smooth, on the nanoscopic level there is a significant amount of surface roughness, which increases the available surface area for reactions to occur. This is true even for polished electrodes; for example, a smooth Pt electrode will typically have an electrochemical surface area (ECSA) approximately two times larger than the geometric area.¹⁴ These quantities are related by the roughness factor, which is simply the ratio of the ECSA to the geometric area,

$$\text{Roughness Factor} = \frac{\text{ECSA}}{\text{Geometric Area}} \quad [1]$$

It is possible to calculate the ECSA (for Pt, harder for other materials) by measuring the amount of a specific species adsorbed to the electrode surface. Common species used are carbon monoxide and hydrogen. In both cases, a cyclic voltammetry experiment is performed over a specific potential range and the current as a function of potential is measured. This current exhibits peaks at potentials where species are adsorbing or desorbing. By integrating the area of the peak and dividing by the scan rate, the total charge of the adsorbed species can be calculated. The surface charge density of the species on the specific electrode material is measured in a separate experiment, and this value can be used to convert the total charge to an ECSA (assuming that the species adsorbs in a monolayer). An example of this approach to ECSA calculation can be seen in work done by Novitski et al., who used a decreasing ECSA with relative humidity to correct mass-transport

measurements.¹⁴ By electroplating the ME surface it is possible to increase the ECSA of the electrode and raise the measured current, as area and current are (in theory) directly proportional as long as the area is accessible by the electrolyte/reactant. The main benefits of this approach are that the higher current is generally more stable, less effected by background electrical noise, and easier to measure. However, this approach becomes problematic when attempting to extract mass-transport parameters (as discussed later) from experimental data. The uncertainty introduced by the larger area relative to the geometric area greatly complicates the numerical model, as the current measured from a plated electrode, while higher than an unplated surface, does not scale as expected with ECSA. Therefore, it is recommended to use a smooth ME in these cells if not hardware limited (lower bound current limit of potentiostat or noise of the system).

Microelectrode preparation including cleaning and casting.—

The ME requires careful handling, preparation, and usage in order to ensure reproducible results and to minimize the impact of contaminants either on the electrode or in the electrolyte or feeds. Due to the small electrode size and very small currents, the threat of contaminants impacting the results is very high. It is advisable to treat the ME and cells with procedures appropriate for ultra-high purity electrochemical measurements, including periodic cleaning of the ME and hardware in strong acids and boiling in ultrapure (18.2 MOhm) water and storing all wetted components in ultrapure water.

The ME itself consists of a metal wire embedded in glass. The tip is cut and polished by the manufacturer. If using the polished ME surfaces for analysis, care must be taken to maintain the polish with a fine alumina polish and appropriate felt pad dedicated to the ME. While with RDE one can polish and visually see the roughness level and imperfections with the naked eye, MEs are too small and require more sophisticated tools. This becomes important if the electrode is plated or there is ionomer casting and/or direct compression with harder surfaces. At a minimum, the surface should be inspected by optical microscope to ensure no obvious pits exist. Scanning electron microscopes (SEMs), atomic force microscopes (AFM), or profilometers can be used for a more detailed surface analysis. For well-studied metals like Pt, cyclic voltammetry in a liquid electrolyte (perchloric or sulfuric acid) can be used to quantify the ECSA and compute a roughness factor. This can be used over the life of the electrode to evaluate how worn-out the surface has become. After polishing, the ME must be cleaned in order to remove the polishing materials and prevent contamination of the electrolyte. Rinsing with an ultrasonic bath in DI water, and a quick submersion in a weak perchloric acid should remove most particle contaminants and oils. The ME should also be stored in an appropriately clean vessel until it is ready to be used; we suggest deionized water.

Casting ionomers on the surface of the ME is a necessity for thin film measurements, but it can also introduce contaminants as the ME will inevitably go through several preparation steps including perhaps an annealing treatment before the electrochemistry is performed. The most basic deposition method is drop casting, where a dilute solution of ionomer in water and solvents is deposited on the surface and allowed to dry. The drying conditions alter the structure and quality of the film and can mitigate or introduce contaminants. The cast film should be dried in a controlled gas environment, protected from particles in the air/room. Once dry, the film can be annealed in a vacuum oven, once again keeping the ME covered to prevent surface contamination. Time, temperature, and vacuum affect the structure of the ionomer film. Subsequently, the electrode can be removed and directly transferred to the ME cell. It may be wise to perform an acid cleaning of the tip, with a rinse in DI water, and a sanity check in a dilute acid ME cell to ensure contaminants are not affecting the response of the ME. These steps may affect the structure and presence of the ionomer film. Post-testing, the ME should be carefully cleaned of the ionomer film by dipping in acid and rinsing with DI water in an ultrasonic bath. An optical microscope is helpful in ensuring the film has been removed.

Additional information surrounding ME preparation can be found in the “Best Practice Guide” in Table III.

Data Analysis

Mass transport to the electrode surface.—Perhaps the most common study performed with MEs and a polymer electrolyte is operation of the cell at mass transport-limiting current to elucidate the solid electrolyte’s mass-transport properties. This is typically performed through chronoamperometry or potential stepping from a low overpotential to a high overpotential in the mass transport-limited region of the polarization curve. The experiment then becomes a classic mass-transport problem, shown in Fig. 3a. It should be noted that this assumes the limiting reactant is coming from the environment through the polymer electrolyte (e.g., water vapor, oxygen, hydrogen, etc.). The current at a given time t is proportional to the flux at the disk surface,

$$I = (AnF) * D \frac{\partial c}{\partial z} \Big|_{z=0} \quad [2]$$

where I is the current, A is the electrode area, D is the diffusivity, c is the gas concentration, F is Faraday’s constant ($96,485 \text{ C mol}^{-1}$), and n is the number of electrons involved in the reaction.¹ This flux is governed by the diffusion equation in the electrolyte,

$$\frac{\partial c}{\partial t} = D \nabla^2 c \quad [3]$$

where t is time.¹ Therefore, a solution to Eq. 3 is needed to determine the current $I(t)$ at the electrode surface.

For a disk, the cylindrical geometry applies intuitively with r and z dependences (θ is cancelled due to symmetry). Equation 3 thus becomes¹

$$\frac{\partial c}{\partial t} = D \left[\frac{1}{r} \frac{\partial}{\partial r} \left(r \frac{\partial c}{\partial r} \right) + \frac{\partial^2 c}{\partial z^2} \right] \quad [4]$$

where one initial and four boundary conditions are needed to fully specify this problem. The initial condition is taken to be $c = c_\infty$ at $t = 0$ (i.e. the electrolyte is fully equilibrated with gas).¹ Because the experiment is at limiting current, the reaction has a negligible impact on the measured current, and thus the concentration of gas at the disk surface is 0 for $t > 0$.¹ There is no flux into the bottom surface outside of the electrode at $t > 0$, giving boundary condition two, and boundary condition three is given by considering that $c \rightarrow c_\infty$ as $r \rightarrow \infty$.¹ The fourth and final boundary condition depends on the geometry of the electrolyte. In the conventional case, z is taken to go to infinity far from the electrode surface, and the boundary condition is then $c \rightarrow c_\infty$ as $z \rightarrow \infty$ (Fig. 3b).¹ There are several solutions available for this formulation. The simplest is a linear equation that is within 7% accuracy of the more exact solutions,

$$I = \frac{nFAD\frac{1}{2}C}{(\pi t)^{\frac{1}{2}}} + 4nFDCR_e \quad [5]$$

where R_e is the electrode radius.¹ A more accurate solution was provided by Aoki and Osteryoung:

$$I = \frac{4nFADC}{\pi R_e} [0.88623\tau^{-\frac{1}{2}} + 0.78540 + 0.094\tau^{\frac{1}{2}}],$$

$\tau < 1$

$$I = \frac{4nFADC}{\pi R_e} [1 + 0.71835\tau^{-\frac{1}{2}} + 0.05626\tau^{-\frac{3}{2}} - 0.00646\tau^{-\frac{5}{2}} + \dots], \tau > 1 \quad [6]$$

where

$$\tau = \frac{4Dt}{R_e^2} \quad [7]$$

This solution is broken up into two regimes for short and long times, with the division at $\tau = 1$.¹ An alternative, empirical solution has been formulated by Shoup and Szabo:

$$I = \frac{4nFADC}{\pi R_e} [0.7854 + 0.8862\tau^{-\frac{1}{2}} + 0.2146e^{-0.7823\tau^{-\frac{1}{2}}}] \quad [8]$$

It is within 0.6% of the solution given by Eq. 6 at all times.¹ More exact solutions do exist but are not typically necessary, as experimental error will exceed any additional accuracy provided by these analytical solutions.²²

These solutions are accurate for the case when the z boundary approaches infinity, which is the typical scenario for an aqueous electrolyte. However, in the solid state, the z -direction will typically extend only on the order of micrometers away from the electrode surface (Fig. 3c). This is problematic, as the fourth boundary condition no longer holds, and thus the solutions above are insufficient to solve the problem. Two primary methods have been proposed to circumvent this issue. The first is to only fit the current-time curve to data over a short time window near the beginning of the experiment.¹⁸ The diffusion field in the electrolyte should be identical to that of the infinite z case at very short times, or until the finite z boundary is reached by the diffusion-field edge. Over this window, the current should follow equations similar to the ones given above.¹⁸ Many studies have been done using this method to fit current-time data to extract diffusivity and solubility.^{14,16–18} However, a significant concern is that the time range over which this fit is performed is arbitrary and will vary depending on the diffusivity calculated, as dimensionless time varies with diffusivity (see Eq. 7). There is no clear experimental evidence demonstrating when the diffusion profile reaches the edge of the electrolyte, and thus the time selected is usually the earliest time data that appears linear and fits the models. The second possible method is to solve for the concentration profile and current numerically. Novitski et al.²³ calculated a numerical solution in their study of the mass transport parameters of alkaline membranes and compared the results with that of the traditional fitting method. Their results showed that the analytical models differed from that of the numerical solution by up to 28.5%, depending on the parameter of interest.

Given the difference in measured parameters between fitting methods, it is difficult to recommend the use of the traditional analytical method of fitting linear short-time data to obtain diffusivity and solubility. It is clear that the assumption of short-time profiles similar to that of the infinite z boundary does not correctly predict the entire transient, perhaps indicating that the finite z boundary has a larger impact on the short-time concentration profile than originally thought. Therefore, we recommend the use of a numerical solution to determine diffusivity and solubility from this type of experiment, as this allows for fitting the entire current transient to improve the accuracy of the reported parameters.²³

Understanding electrochemical kinetics with MEs.—In addition to obtaining transport properties, MEs can also be used to evaluate kinetic parameters of electrochemical reactions. These parameters include the exchange current density (i.e. the electron-transfer rate constant of an electrochemical reaction analogous to the rate constant for a chemical reaction) and the Tafel slope. These parameters often are written in the form of an overall Butler-

Table III. Author suggestions for working with microelectrode setups.

Category	Author Recommendations
Materials/ Hardware	<ul style="list-style-type: none">• Ensure that the microelectrode cell has been boiled recently to remove lingering impurities.
Assembly	<ul style="list-style-type: none">• Use a new membrane and new counter electrode (if not using a platinum mesh) for each experimental setup.• Clean (with DI water) and dry (with nitrogen) the microelectrode tip before use.• Use a membrane equilibrated with ambient humidity (if working with PFSA) to ensure drying from liquid-equilibrated conditions does not cause the membrane to lift off the electrodes.• Ensure that the membrane is cut in such a way that the reference pin touches the counter electrode, not the membrane.• Before assembly, apply a few drops (~2) of the relevant ionomer dispersion to the microelectrode tip. This will create an adhesion layer upon assembly and drying that will seal the edges of the microelectrode and not allow gas to bypass the membrane.• It is simple to confirm that the seal has worked. Upon assembly and testing, check the magnitude of the current vs an expected current calculation. If the current is multiple orders of magnitude higher (e.g., μA vs nA) the seal has not worked, leakage is occurring, and the cell must be rebuilt.
Testing	<ul style="list-style-type: none">• Due to room noise and other fluctuations, it is helpful to operate the potentiostat with a manual ground (as opposed to allowing the potentiostat to set its own ground). The ground can simply be the Faraday cage used to shield the cell. (Note: aluminum foil is an effective Faraday cage).

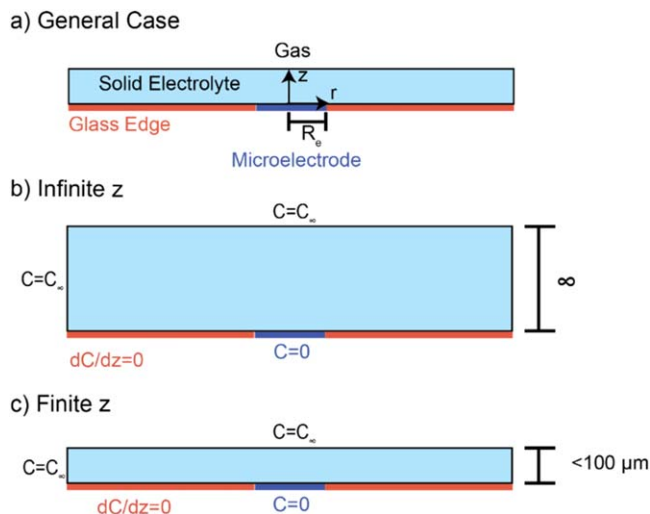


Figure 3. (a) shows the general problem setup for MEs with a polymer electrolyte, while (b) shows the infinite z case and (c) shows the finite z case.

Volmer equation (Eq. 9); although more complicated microkinetic models can be used, such discussion is beyond the scope of this tutorial.²⁴

$$i = i_0 \left[\exp\left(\frac{\alpha_a F}{RT} \eta_s\right) - \exp\left(-\frac{\alpha_c F}{RT} \eta_s\right) \right] \quad [9]$$

where i is the current density, i_0 is the exchange current density, α_c is the symmetry factor which equals the fraction of applied voltage which corresponds to the cathodic half reaction, α_a corresponds to the fraction which corresponds to the anodic half reaction and is equal to $1 - \alpha_c$, R is the ideal gas constant, T is the temperature, and η_s is the surface overpotential. In the case of high overpotential, the expression simplifies to

$$i = i_0 \exp\left(\frac{\alpha_a F}{RT} \eta_s\right) \quad [10]$$

which can be converted into a linear form,

$$\ln(i) = \frac{\alpha_a F}{RT} \eta_s + \ln(i_0) \quad [11]$$

This relationship can be used to calculate the exchange current density through a Tafel plot, which is a plot of η_s vs. $\log(i)$. The exchange current density is equal to 10 raised to the power of the x -intercept of the Tafel plot extrapolated from the linear region that occurs at large η_s . Another useful parameter that can be extracted is the Tafel slope, which is the slope of linear region used to calculate the exchange current density. The Tafel slope is equal to $2.303RT/\alpha_a F$, and gives useful information about the symmetry factor for the reaction, and is understood to be related to the reaction mechanism.

The above analysis is valid for cases of high overpotentials, or where the reaction is not very reversible. For low surface overpotentials, the Butler-Volmer equation can be approximated as

$$i = i_0 \frac{(\alpha_a + \alpha_c) F}{RT} \eta_s \quad [12]$$

In addition, it is possible to achieve very high rates of diffusion at the surface of a ME, which allows for reactions of very short lifetime (on the order of tens of nanoseconds) to be analyzed.⁹ This makes MEs a very useful tool for analyzing rapid kinetics. High-speed cyclic voltammetry can be used to obtain the rate constant for heterogeneous electron-transfer by examining how the separation of the oxidation and reduction peaks changes with scan rate.⁹ The rate

constant can also be extracted from steady-state slow scanning cyclic voltammetry, which simplifies corrections and equipment requirements. The kinetics of fast reactions can be also be deduced using cyclic voltammetry at very low temperatures.²⁵ In addition, MEs allow for electrochemical studies of the microsecond regime through potential step methods and other experimental approaches.¹ It is theoretically possible to use MEs to conduct studies in the even shorter nanosecond regime; however, it requires the electrode size to be reduced and the electrolyte to have high conductivity.¹ One of the fastest studies in which diffusion occurs that has been conducted using MEs is in the timescale range of 500 ns, showing the potential for this type of measurement.¹

Polymer-Electrolyte Microelectrode Applications

The studies performed using ME polymer-electrolyte cells can be grouped into two main categories: mass-transport parameters and electrochemical reaction. Due to the field's primary association with fuel-cell polymer membranes, oxygen and hydrogen gas have been the most widely studied, particularly oxygen, along with the associated electrochemical HOR and ORR.^{14,18,20,26} However, the focus has broadened more recently to include polymers beyond Nafion such as other PFSA membranes and alkaline membranes.^{23,27,28} Thin films (<100 nm) of Nafion have also been compared to micrometer-thick membranes (such as N117 or N211), allowing for an in-depth study of interface properties of thin ionomer films compared to bulk membrane properties.¹⁶ In addition, MEs can be used to study the impact of various environmental effects in systems that mimic high temperature PEMFCs.²⁹ This section examines all key areas of the literature, highlighting the most important studies from each.

Mass-transport studies.—The first modern polymer-electrolyte ME cell was developed by Parthasarathy et al. in 1991 and subsequently used for various studies.^{8,18} This was the first paper to report the mass-transport properties of oxygen in Nafion as well as details on the kinetics of the ORR reaction in a polymer electrolyte via the ME interface. In their initial study, 175 μm thick Nafion 1100 was used with a 100 μm diameter Pt ME under one set of conditions: 99.9% RH, 24.5 $^\circ\text{C}$, and 1 atm. The authors also pioneered the analysis method used in nearly every subsequent study, where an analytical solution for the $I(t)$ curve in the infinite z domain was fit over a short early-time range of the experimental data to determine mass-transport properties (see Fig. 4), although with the caveats discussed in the previous section.¹⁸ Equation 5 was used to fit the data due to its simplicity and relative accuracy. Oxygen gas was shown to have a diffusion coefficient of $7.4 \times 10^{-7} \text{ m}^2 \text{ s}^{-1}$ and a solubility of 26 mM in Nafion.¹⁸ Despite the long equilibration times and laborious setup, this work showed that these parameters could be determined accurately and consistently using MEs and polymer electrolytes.¹⁸

In PEMFC operation, performance under reduced RH conditions is quite important and ME cells can be used to study this as well. Novitski and Holdcroft¹⁴ applied MEs to the study of oxygen transport in Nafion with relative humidities lower than 100%. Unlike other setups, the cell design here was two-electrode and used a 5 μm Pt electrode, with Nafion 211 (25 μm thick) and a deposited solution of DE2020 as electrolytes. An identical fitting method to Parthasarathy was used, although the time domain used was significantly shorter ($0.5 < \tau < 1$).¹⁴ In addition, the Shoup-Szabo equation was used (Eq. 8). The authors found that as humidity decreased, diffusivity and permeability decreased while solubility increased (see Fig. 5).¹⁴ This supports previous theories that most gas transport occurs in the water phase of the membrane even though the gas is more soluble in the polymer phase of the membrane.³⁰ However, the authors also found that the answers reported by the two different fitting methods differed by over an order of magnitude, casting doubt on the accuracy of the analytical fitting techniques.¹⁴

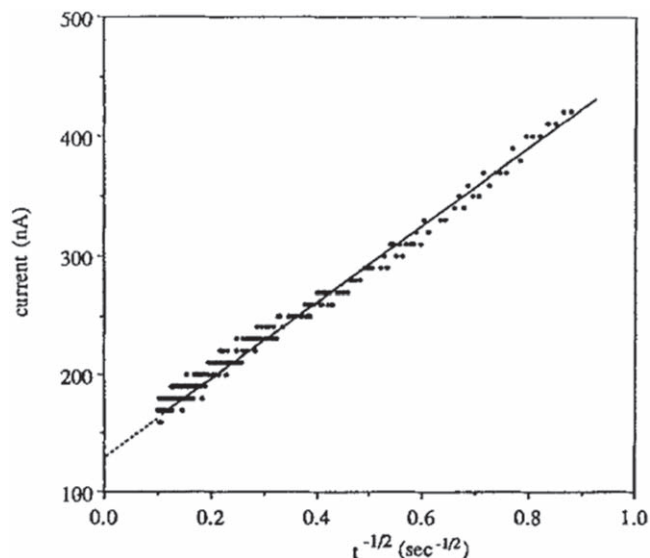


Figure 4. Plot of experimental current vs $t^{-1/2}$ from Parthasarathy et al. over a limited time range, fit using Eq. 5.¹⁸ A. Parthasarathy, C. R. Martin and S. Srinivasan, *Journal of The Electrochemical Society*, **138**, 916 (1991). © IOP Publishing. Reproduced with permission. All rights reserved.

that for very thin films, the interfacial resistance is equivalent to adding another 30 to 70 nm of film.¹⁶ This is important for applications that use Nafion films of <100 nm, as this will impose a lower limit on the resistance despite reduction of film thickness below 30 nm. The study also concluded, in support of previous work, that permeability and diffusivity of oxygen gas tend to increase with increasing RH, while solubility decreases, and this is consistent for the interfacial resistance as well.

The study of oxygen transport in polymer membranes using MEs has been extended beyond Nafion to include other PFSA polymers, including BAM3G 407 and 6F-40.^{17,15} Basura et al.¹⁷ compared oxygen transport in Nafion 117 (190 μm) and BAM3G 407 (140 μm), using a 50 μm Pt electrode in both cases at 30 $^{\circ}\text{C}$ and 3 atm of O_2 as well as 100% RH. Interestingly, they concluded that while the permeabilities of the membranes were nearly identical ($\sim 55 \times 10^{-12} \text{ mol cm}^{-1} \text{ s}^{-1}$), the BAM3G 407 membrane had a diffusion coefficient about 4 times larger than that in Nafion 117, but that the solubility of oxygen in Nafion 117 was about 4 times larger than in the BAM3G 407. This was attributed to the higher water content of the BAM membrane, providing additional evidence that oxygen transport occurs primarily in water but that it dissolves much easier into the polymer backbone.³⁰ Chlistunoff studied the mass-transport properties of oxygen in 6F-40, a membrane similar to Nafion but with a more beneficial morphology.¹⁵ The study was performed using 26.5 μm films of 6F-40 on a 100 μm Pt ME at 20 $^{\circ}$

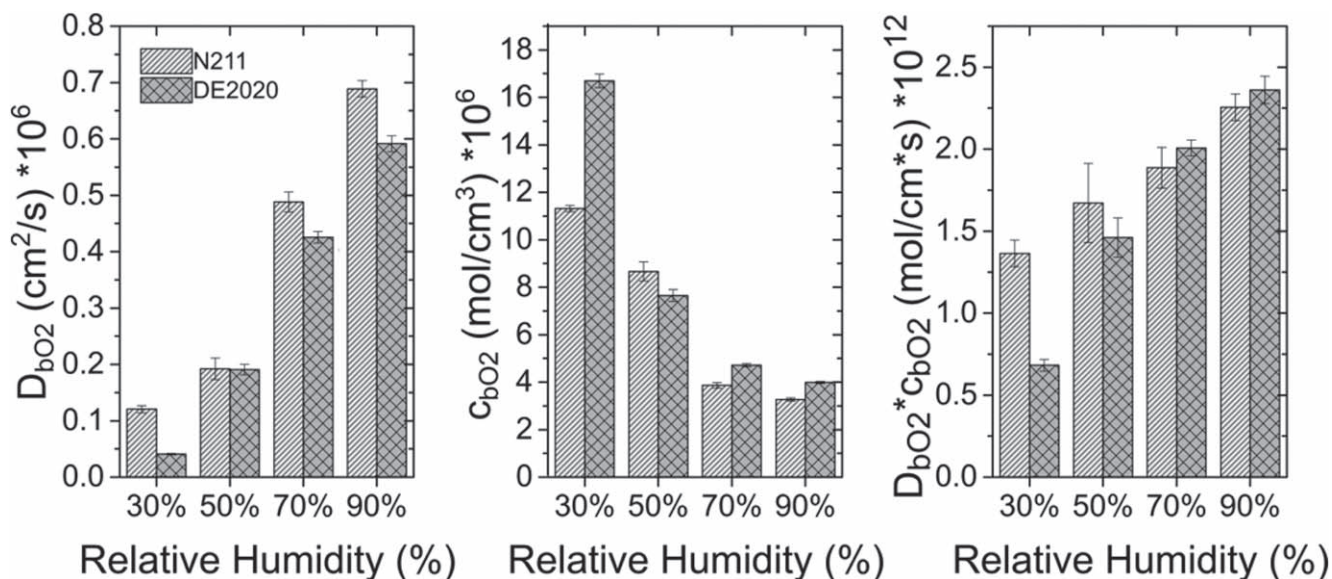


Figure 5. Compiled mass-transport parameters for oxygen in Nafion ionomer layers as a function of relative humidity from reference.¹⁴ Reprinted with permission from D. Novitski and S. Holdcroft, *ACS Appl Mater Interfaces*, **7**, 27314 (2015). Copyright 2015 American Chemical Society.

Due to their small size and low measured currents, MEs can also be used to measure the interface resistances of thin films. Kudo et al.¹⁶ cast thin films of Nafion using 0.3–0.7 wt.% solutions, resulting in films 20 to 100 nm in thickness, and compared the results for oxygen transport with those obtained from 100 μm membranes. To determine the interfacial resistance, a linear expression for the oxygen transport resistance was derived,

$$R_{\text{O}_2} = \frac{nFc_{\text{gas}}}{i_d} = \frac{1}{RTDK_H}x_0 + \frac{1}{RTK_H} \left(\frac{1}{k_{\text{Pt}}} + \frac{1}{k_{\text{ion}}} \right) \quad [13]$$

The term $\frac{1}{K_H} \left(\frac{1}{k_{\text{Pt}}} + \frac{1}{k_{\text{ion}}} \right)$ is the sum of the interfacial resistances on the Pt/ionomer and ionomer/gas sides of the film, respectively.¹⁶ The current-time curves for the 100 μm membrane were fit by the method described by Parthasarathy et al. The authors concluded

C and 60% RH, finding the diffusion coefficient of oxygen to be $4.5 \times 10^{-8} \text{ cm}^2 \text{ s}^{-1}$ and the solubility to be $9.8 \times 10^{-6} \text{ mol cm}^{-3}$.¹⁵ The permeability was $4.4 \times 10^{-13} \text{ mol cm}^{-1} \text{ s}^{-1}$. Data were fit using both an equation similar to Eq. 5 and as well as Eq. 8. This study once again shows the flexibility of MEs for studying polymer membranes.

Novitski et al.²³ went further, abandoning the PFSA acidic electrolyte environment entirely to test the mass-transport parameters of an alkaline membrane, hexamethyl-p-terphenyl polymethylbenzimidazoles (HMT-PMBI) and compare them to FAA-3, an alkaline membrane from FuMA-Tech GmbH. This work used a 53 μm thick membrane of HMT-PMBI and a 5 μm Pt ME, performing all tests using air at varying humidities and 60 $^{\circ}\text{C}$. Multiple films of HMT-PMBI were formulated to test different ion-exchange capacities. The Shoup-Szabo equation (Eq. 8) was used to fit the current-time curve to extract the diffusivity and solubility. The authors found that, similar to PFSA membranes, oxygen diffusivity and permeability increase with humidity while

solubility decreases for both the FAA-3 and HMT-PMBI.²³ In addition, the HMT-PMBI showed higher diffusivities and permeabilities at all humidities compared to FAA-3, while the FAA-3 showed higher solubilities at all humidities. Alternatively, membranes with higher ion exchange capacities (and therefore higher water content) demonstrated higher diffusivities and permeabilities but lower solubilities. Compared to Nafion, both alkaline membranes performed better at higher humidities but worse at lower humidities, leading to the conclusion that transport performance was even more water content dependent than it is in Nafion.

To this last point, only the transport parameters for oxygen have been discussed. However, it is possible to study other gases, such as hydrogen. Jiang and Kucernak²⁶ leveraged the hydrogen oxidation reaction on Pt to study the mass-transport hydrogen in Nafion. A 50 μm Pt-plated gold electrode was used with Nafion 117 as the electrolyte membrane. An equation similar to equation 5 was used to fit the current-time curve over the range $0.2 < \tau < 100$ (see Fig. 6).²⁶ The authors found that at 20 °C, the diffusion coefficient of hydrogen was $7.6 \times 10^{-6} \text{ cm}^2 \text{ s}^{-1}$, the solubility was $0.51 \times 10^{-6} \text{ mol cm}^{-3}$, and the permeability was $3.9 \times 10^{-12} \text{ mol cm}^{-1} \text{ s}^{-1}$.²⁶ As temperature increased, the study showed that diffusivity and permeability increased, while solubility demonstrated an inconsistent trend.²⁶ The trends for diffusivity and permeability with temperature align with the results that have been reported for oxygen.^{14,16,26}

The effect of polymer equivalent weight on all of the previously described mass-transport parameters can be easily studied as an extension of the prior works. Buchi et al.²⁸ examined two different types of PFSA membranes: Aciplex and Nafion, to determine the impact of equivalent weight (and perhaps the side-chain length).³⁰ Equivalent weight varied from 880 to 1200 g mol^{-1} , with 5 different samples tested.²⁸ The current-time data was fit with an equation similar to Eq. 5, as has been done previously; however, the early time data was excluded in this case due to nonlinear behavior at short times.²⁸ This behavior was attributed to surface oxide reduction, but the true cause is unclear. The authors conclude that oxygen diffusivity decreases with increasing equivalent weight, while solubility increases over the same range. Permeability exhibited no definitive trend other than Aciplex having a much higher permeability than Nafion.²⁸ Basura et al.²⁷ performed a similar study with BAM and DAIS polymer membranes. BAM is a sulfonated α , β , β -trifluorostyrene-co-substituted- α , β , β -trifluorostyrene, while the DAIS polymers are sulfonated styrene-(ethylene-butylene)-styrene copolymers. Experiments were performed in a similar manner as other studies, using a 50 μm Pt ME and fit with an equation similar to Eq. 5 over a limited, early-time window.²⁷ Similar to Buchi et al., the authors found that oxygen diffusivity decreases with increasing equivalent weight, while solubility increases. Contrary to the previous work, permeability was found to decrease with increasing equivalent weight, as the drop in diffusivity is higher than the increase in solubility. Taken together, both studies show that the aqueous phase, which increases as equivalent weight decreases, has a large role in the diffusion pathways of oxygen through polymer membranes. In addition, the solubility is much more dependent on the polymer backbone than on the water phase. Examination of these properties was relatively straightforward as a simple extension of previous work and highlights the flexibility of polymer-electrolyte ME cells for studying a wide variety of experimental conditions.

Reaction studies.—There are many experimental benefits of the ME system, which allows for greater understanding of reaction kinetics and the ability to extract kinetic parameters. A variety of different electrochemical reactions have been analyzed using MEs. Among these, the reactions that have been the most extensively studied are ORR and HOR, with ORR the more explored reaction, enabled by its importance in PEMFCs and sluggishness. As mentioned above, Parthasarathy et al.¹⁸ pioneered a ME cell design that enabled testing the ORR using a solid polymer electrolyte. In addition to evaluating parameters for transport through the

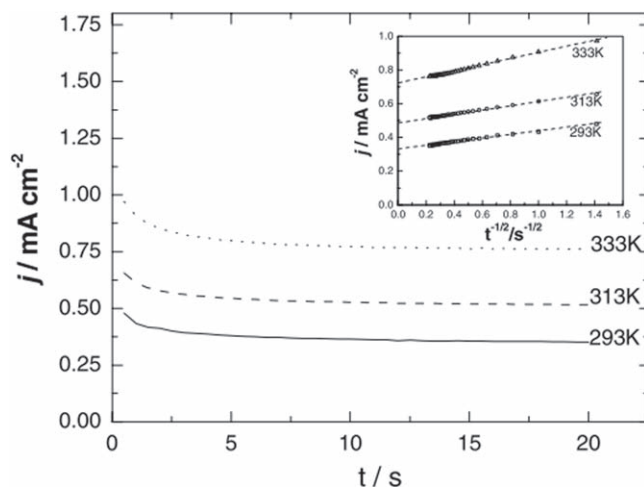


Figure 6. Current density-time curves for the HOR at a Pt electrode (inset: current density vs $t^{-1/2}$). Results are quite similar in trend as for oxygen, and the linearity of the plot in the inset is quite clear.²⁶ This figure was published in the Journal of Electroanalytical Chemistry, 567, J. Jiang and A. Kucernak, Investigations of fuel cell reactions at the composite microelectrode/solid polymer electrolyte interface. I. Hydrogen oxidation at the nanostructured Pt|Nafion® membrane interface, 123–137, Copyright Elsevier (2004).

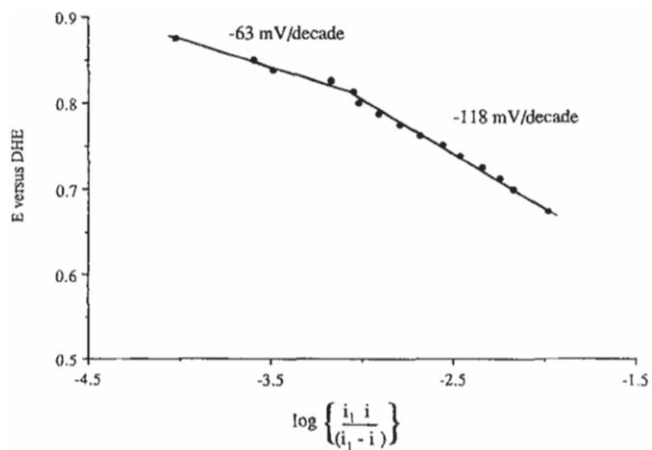


Figure 7. Tafel plot that has been mass transfer corrected for the oxygen reduction reaction occurring on Pt with Nafion, depicting two distinct regions, reproduced from Ref. 18. A. Parthasarathy, C. R. Martin and S. Srinivasan, Journal of The Electrochemical Society, 138, 916 (1991). © IOP Publishing. Reproduced with permission. All rights reserved.

membrane, this setup also determined kinetic parameters of interest, such as the Tafel slope and the exchange current density for ORR.^{31–33} Using their setup, they found two distinct regions in the Tafel plot with Tafel slopes of -119 and $-63 \text{ mV decade}^{-1}$ (as shown in Fig. 7), with corresponding exchange current densities of 7.8×10^{-7} and $2.05 \times 10^{-9} \text{ A cm}^{-2}$, respectively. These distinct regions imply different adsorption isotherms and rate-determining steps over the potential range examined. Uribe et al.²⁰ studied ORR to better understand the Pt/Nafion film interface in PEMFCs and found that performance dropped significantly as the membrane dried out, and conjectured that it was due to ionomer surface restructuring. Additionally, Uribe found that the Tafel slope was not constant when the potential was greater than 0.7 V. Below 0.7 V, the Tafel slope was 180 mV/decade.²⁰

HOR began to be studied using MEs a little over a decade after the initial ORR studies. Following ORR catalyst improvement, HOR catalyst studies were important for trying to improve PEMFC performance and decrease capital cost from catalysts. Jiang et al.²⁶ pioneered the approach to characterizing electrocatalyst performance

using high roughness MEs to study HOR. Using this technique, they hoped to study PEMFC catalyst performance under conditions similar to normal operating conditions, evaluating the catalyst at the interface of a solid polymer electrolyte without any supporting aqueous electrolyte. They were able to evaluate the mass transport in solid electrolytes, electrode kinetics, and intrinsic activity of electrocatalysts using cyclic voltammetry at 200 mV s^{-1} to evaluate the catalyst electrochemically active surface area, and slow linear sweep voltammetry was used to evaluate the kinetics of the reaction using a scan rate of 5 mV s^{-1} . They observed an experimental Tafel slope of $33 \text{ mV decade}^{-1}$ and an exchange current density of 0.2 mA cm^{-2} for HOR on Pt in contact with Nafion 117 at 20°C .²⁶

Another area that MEs can be helpful is in elucidating reaction mechanisms. Quaino et al.³⁴ used experimental data evaluating HOR on Pt MEs to evaluate the mechanistic pathway of HOR. This study collected experimental data to extract kinetic parameters based on the proposed elementary HOR reaction steps following the Tafel-Heyrovsky-Volmer mechanism. The kinetic model had very good agreement with the collected experimental data, supporting the proposed mechanism.

MEs can also be used to study reactions kinetics in an alkaline environment, either using an aqueous alkaline electrolyte or an alkaline membrane and ionomer in a solid-state system. There is great interest in studying electrochemical reactions under alkaline conditions because many non-precious catalysts are stable under high pH conditions with changing potential, where they would rapidly dissolve under acidic conditions.³⁵ This opens up the possibility of implementing lower cost catalysts to reduce system costs. A study by Arce et al.³⁶ used Pt MEs to study the HER across pH ranges from acidic to alkaline. In this study, kinetic rate parameters for HER were determined for acidic and alkaline solutions based on the Volmer–Heyrovsky–Tafel mechanism. From these experiments, under alkaline conditions ($\text{pH} = 10.8$) it was found that the exchange current density was $1.02 \times 10^{-3} \text{ A cm}^{-2}$ for HER on Pt, compared to $85 \times 10^{-3} \text{ A cm}^{-2}$ under acidic conditions ($\text{pH} = 3.6$).³⁶ Additionally, it was found that the calculated kinetic parameters used to model the reaction rate in acidic solutions did not accurately model the reaction for alkaline solutions, and other kinetic parameters were used to model the alkaline reaction. The reason for this could be attributed to change in electrode behaviour in alkaline solutions, fouling from contaminants, or oversimplification in the model.

Additional applications.—Recent studies have expanded ME use to study catalyst-ionomer interactions.²¹ These studies include work by Gunasekara et al. which employed a solid state electrochemical cell with a Pt ME to probe alkaline HOR and the methanol oxidation reaction. It was found that a film of AS-4 ionomer significantly decreased the rate of HOR due to carbonate ion adsorption.³⁷ A study by Helmlly et al. studied the rate of ionomer decomposition and local reaction conditions on performance in a multilayer PEM cell using a Pt ME.³⁸ Maurya et al. studied undesirable phenyl group interactions of a polyaromatic ionomer with Pt-Ru/C microelectrodes, and used the gathered information to design a new ionomer which greatly improved the peak power density for alkaline HOR.³⁹ These studies emphasize that MEs can also be used to interrogate interfaces and remain an area of burgeoning and active research.

Another fruitful application of MEs is in studying very fast reactions by using cyclic voltammetry with high scan rates (up to 10^5 to 10^6 V s^{-1}).⁴⁰ The advantage of these measurements is that the time scale reaches the magnitude of μs , which can be used to determine rate constants for fast charge transfer reactions and to better understand mechanisms. Studies done by the McCreery group were the first to use these techniques, and achieved a response time of approximately $30 \mu\text{s}$.⁴¹ They determined that the rate constant for the reduction of the chlorpromazine cation radical (CPZ^+) species by dopamine to be $6.2 \times 10^7 \text{ l mol}^{-1} \text{ s}^{-1}$ by using chronoamperometric measurements at a pH of 6.8.⁴² These results illustrate the

advantages of MEs for analyzing the kinetics of fast electrochemical reactions.

Summary and Future Directions

Studying polymer electrolytes and the ionomer/electrode interface with microelectrodes is still an underdeveloped, yet important aspect of modern electrochemistry. Progress has been slow and disjointed, and it is only recently that the available body of research has expanded to include somewhat basic studies such as numerical modeling of diffusion in the membrane. However, significant progress has been made recently with the developments by several groups in the last few years on new types of membranes and true thin films. Care must be taken in both the data acquisition and the data analysis, especially in terms of understanding mass transport and the impact of contaminants.

There are several different directions in which the field can proceed. One significant area of growth is in the standardization and improvement of ME studies. On the hardware side, even with recent improvements, many ME cells lack efficiency (e.g. long equilibration times) and/or features to improve accuracy, such as having a dedicated reference electrode. As these designs mature, it will become easier to study other aspects of membrane performance, such as with non-Nafion thin films and membranes, doped ionomers, other reactions and electrode materials. On the analysis side, improvements in the modeling of gas transport in the ionomer membrane are critical for determining accurate parameters. Another common PEMFC study is an accelerated stress test (AST). By properly treating the ionomer prior to use with the ME, the ionomer/electrode interface could be examined under conditions of extreme degradation, which would give insight into the fail points of the interface. Understanding these different environmental conditions is critical for improving the efficiency and performance of PEMFCs.

Most of the work to date has been applied towards PEMFCs; electrolyzers and electrosynthesis remain relatively unexplored areas upon which MEs can make great strides in elucidating mechanistic studies and kinetic parameters in gaseous environments. This is especially true as the ionomer/electrode interface and the local environment are increasingly being seen as the key attribute for these reactions. By simply switching the electrode from Pt to something more suitable for these reactions, such as gold, copper, or iridium, it would be relatively straightforward to study these reactions. This is perhaps the most immediate progress that will be seen in the near future. Another rising technology is solid-state batteries. MEs could provide a valuable diagnostic tool for studying the polymer or ceramic electrolytes in these systems outside of the batteries themselves. With some modification and use in a controlled environment, most of the ME cell designs could be used with lithium electrodes, the preferred material for these solid-state batteries. Finally, CO_2 reduction and electrochemical fuels production is an emerging field of study in which solid polymer electrolytes are used. In this case, the reactants and products can change the local pH environment of these solid electrolytes, and the resolution of products and faradaic efficiencies must be done with a fast response time. MEs could be used to resolve these issues and study the kinetics of CO_2 reduction with solid electrolytes.

Acknowledgments

The authors acknowledge funding from the Million Mile Fuel Cell Truck (M^2FCT) Consortium, funded by the Department of Energy—Office of Energy Efficiency and Renewable Energy—Hydrogen and Fuel Cell Technologies Office (DOE-EERE-HFCTO) under Contract Number DE-AC02-05CH11231, GA acknowledges funding by the National Science Foundation Graduate Research Fellowship Program under Grant No. DGE 1752814, and ND and DIK acknowledge support from the Toyota Motor Company. Any opinions, findings, and conclusions or recommendations expressed in this material are those of the author (s) and do not necessarily reflect the views of the National Science

Foundation. The authors would like to acknowledge Ahmet Kusoglu on beautification of Figure 1.

ORCID

John G. Petrovick  <https://orcid.org/0000-0003-1607-1455>
 Grace C. Anderson  <https://orcid.org/0000-0002-2723-5024>
 Douglas I. Kushner  <https://orcid.org/0000-0002-3020-7737>
 Nemanja Danilovic  <https://orcid.org/0000-0003-2036-6977>
 Adam Z. Weber  <https://orcid.org/0000-0002-7749-1624>

References

1. A. J. Bard and L. R. Faulkner, *Electrochemical Methods: Fundamentals and Applications* (John Wiley & Sons, Inc, New York) (2001).
2. J. O. M. Bockris, A. K. N. Reddy, and M. E. Gamboa-Aldeco, *Modern Electrochemistry 2A: Fundamentals of Electrode Processes* (Springer, United States of America) (2000).
3. D. Higgins, C. Hahn, C. X. Xiang, T. F. Jaramillo, and A. Z. Weber, *ACS Energy Lett.*, **4**, 317 (2019).
4. S. Nitopi et al., *Chem. Rev.*, **119**, 7610 (2019).
5. A. Z. Weber and A. Kusoglu, *J. Mater. Chem. A*, **2**, 17207 (2014).
6. A. A. Kulikovskiy and P. Berg, *J. Electrochem. Soc.*, **162**, F843 (2015).
7. S. Srinivasan, O. A. Velev, A. Parthasarathy, D. J. Manko, and A. J. Appleby, *J. Power Sources*, **36**, 299 (1991).
8. A. Parthasarathy, B. Dave, S. Srinivasan, A. J. Appleby, and C. R. Martin, *J. Electrochem. Soc.*, **139**, 1634 (1992).
9. R. J. Forster, *Chem. Soc. Rev.*, **23**, 289 (1994).
10. M. Steimecke, G. Seiffarth, and M. Bron, *Anal. Chem.*, **89**, 10679 (2017).
11. D. Polcari, P. Dauphin-Ducharme, and J. Mauzeroll, *Chem. Rev.*, **116**, 13234 (2016).
12. W. Liu and D. Zuckerbrod, *J. Electrochem. Soc.*, **152**, A1165 (2005).
13. Y. Qiao, Y. Qiao, L. Zou, C. Ma, and J. Liu, *Bioresour. Technol.*, **198**, 1 (2015).
14. D. Novitski and S. Holdcroft, *ACS Appl. Mater. Interfaces*, **7**, 27314 (2015).
15. J. Chlistunoff, *J. Power Sources*, **245**, 203 (2014).
16. K. Kudo, R. Jinnouchi, and Y. Morimoto, *Electrochim. Acta*, **209**, 682 (2016).
17. V. I. Basura, P. D. Beattie, and S. Holdcroft, *J. Electroanal. Chem.*, **458**, 1 (1998).
18. A. Parthasarathy, C. R. Martin, and S. Srinivasan, *J. Electrochem. Soc.*, **138**, 916 (1991).
19. J. G. Petrovick, D. I. Kushner, M. Tesfaye, N. Danilovic, C. J. Radke, and A. Z. Weber, *ECSS Trans.*, **92**, 77 (2019).
20. F. A. Uribe, T. E. Springer, and S. Gotesfeld, *J. Electrochem. Soc.*, **139**, 765 (1992).
21. S.-D. Yim, H. T. Chung, J. Chlistunoff, D.-S. Kim, C. Fujimoto, T.-H. Yang, and Y. S. Kim, *J. Electrochem. Soc.*, **162**, F499 (2015).
22. C. A. Basha and L. Rajendran, *Int. J. Electrochem. Sci.*, **1**, 268 (2006).
23. D. Novitski, A. Kosakian, T. Weissbach, M. Secanell, and S. Holdcroft, *J. Am. Chem. Soc.*, **138**, 15465 (2016).
24. J. Newman and K. Thomas-Alyea, *Electrochemical Systems* (Wiley, New York, NY) (2004).
25. W. J. Bowyer, E. E. Engelman, and D. H. Evans, *J. Electroanal. Chem. Interfacial Electrochem.*, **262**, 67 (1989).
26. J. Jiang and A. Kucernak, *J. Electroanal. Chem.*, **567**, 123 (2004).
27. V. I. Basura, C. Chuy, P. D. Beattie, and S. Holdcroft, *J. Electroanal. Chem.*, **501**, 77 (2001).
28. F. N. Büchi, M. Wakizoe, and S. Srinivasan, *J. Electrochem. Soc.*, **143**, 927 (1996).
29. S. Zhang, J. Zhang, Z. Zhu, P. Liu, F. Cao, J. Chen, Q. He, M. Dou, S. Nan, and S. Lu, *J. Power Sources*, **473**, 228616 (2020).
30. A. Kusoglu and A. Z. Weber, *Chem. Rev.*, **117**, 987 (2017).
31. A. Parthasarathy, S. Srinivasan, A. J. Appleby, and C. R. Martin, *J. Electrochem. Soc.*, **139**, 2530 (1992).
32. A. Parthasarathy, S. Srinivasan, A. J. Appleby, and C. R. Martin, *J. Electroanal. Chem.*, **339**, 101 (1992).
33. A. Parthasarathy, S. Srinivasan, A. J. Appleby, and C. R. Martin, *J. Electrochem. Soc.*, **139**, 2856 (1992).
34. P. M. Quaino, J. L. Fernández, M. R. Gennero de Chialvo, and A. C. Chialvo, *J. Mol. Catal. A: Chem.*, **252**, 156 (2006).
35. U. Martinez, S. K. Babu, E. F. Holby, H. T. Chung, X. Yin, and P. Zelenay, *Adv. Mater.*, **31**, 1806545 (2019).
36. M. D. Arce, H. L. Bonazza, and J. L. Fernández, *Electrochim. Acta*, **107**, 248 (2013).
37. I. Gunasekara, I. Kendrick, and S. Mukerjee, *J. Electrochem. Soc.*, **166**, F889 (2019).
38. S. Helmly, M. J. Eslamibidgoli, K. A. Friedrich, and M. H. Eikerling, *Electrocatalysis*, **8**, 501 (2017).
39. S. Maurya, S. Noh, I. Matanovic, E. J. Park, C. Narvaez Villarrubia, U. Martinez, J. Han, C. Bae, and Y. S. Kim, *Energy Environ. Sci.*, **11**, 3283 (2018).
40. J. Heinze, *Angew. Chem. Int. Ed. Engl.*, **32**, 1268 (1993).
41. R. S. Robinson and R. L. McCreery, *Anal. Chem.*, **53**, 997 (1981).
42. R. S. Robinson and R. L. McCreery, *J. Electroanal. Chem. Interfacial Electrochem.*, **182**, 61 (1985).